China's Rainfall Interannual Predictability: Dependence on the Annual Cycle and Surface Anomalies

XIN-ZHONG LIANG

Illinois State Water Survey, Illinois Department of Natural Resources, Champaign, and University of Illinois at Urbana–Champaign, Urbana, Illinois

ARTHUR N. SAMEL

Geography/Environmental Programs, Bowling Green State University, Bowling Green, Ohio

WEI-CHYUNG WANG

Atmospheric Sciences Research Center, University at Albany, State University of New York, Albany, New York

17 August 2001 and 14 January 2002

ABSTRACT

China's rainfall interannual predictability is generally believed to depend upon the accurate representation of its annual cycle as well as teleconnections with planetary surface anomalies, including tropical east Pacific sea surface temperature and Eurasian snow and soil moisture. A suite of general circulation model (GCM) simulations is used to ascertain the existence of these relationships. First, a comparison of thirty 1980–88 Atmospheric Model Intercomparison Project (AMIP) GCM simulations shows no clear correspondence between model skill to reproduce observed rainfall annual cycle and interannual variability. Thus, accurate representation of either component does not ensure the realistic simulation of the other. Second, diagnosis of the 1903–94 and 1950–97 National Center for Atmospheric Research (NCAR) Community Climate Model, version 3 (CCM3), ensemble integrations indicates the existence of teleconnections in which spring planetary surface anomalies lead China's summer rainfall variations. These teleconnections, however, are sensitive to initial conditions, which define distinct dynamic regimes during the integration period. In addition, analysis of the NCAR Climate System Model (CSM) 300-yr equilibrium simulation reveals that the teleconnections display decadal variations. These results cast doubt on the traditional physical mechanisms that explain China's rainfall teleconnections and, hence, emphasize the need to incorporate interactions between planetary surface anomalies and specific dynamic regimes.

1. Introduction

Ideally, to predict China's monsoon rainfall, a GCM must realistically simulate both the annual cycle and interannual variations. Current GCMs, however, do not meet this standard because both components suffer from important model biases (Liang et al. 1995a, 2001; Wang et al. 1998; Liang and Wang 1998). A key issue then arises regarding the credibility of models that poorly reproduce the annual cycle to predict interannual variability. This is further complicated by the fact that the impact of surface anomalies on China's precipitation prediction can be masked by climate system internal natural variability (Fennessy and Shukla 1991; Palmer and Anderson 1994; Liang et al. 1997; Lau et al. 2000). The purpose of this study is to investigate the dependence of China's rainfall interannual variations on the annual cycle and planetary surface anomalies.

Several studies have suggested that GCM-simulated interannual variability is more realistic when model representation of the climate ''mean state'' improves (Palmer and Mansfield 1986; Fennessy et al. 1994; Sperber and Palmer 1996; Gadgil and Sajani 1998; Sperber et al. 1999). This concept, however, has been broadly defined where different fields were analyzed to assess the mean state and interannual variations. We believe that, when a single field is considered, the relationship is climate regime dependent and holds only if both the mean annual cycle and interannual variations are dominated by similar physical processes. In this regard, we will focus on the east China summer monsoon and analyze simulations from 30 Atmospheric Model Inter-

Corresponding author address: Dr. Xin-Zhong Liang, Illinois State Water Survey, 2204 Griffith Dr., Champaign, IL 61820-7495.
E-mail: xliang@uiuc.edu

comparison Project (AMIP) GCMs (Gates et al. 1999) to explore whether a model with a realistic rainfall annual cycle can also predict its interannual variability.

Numerous studies have shown that east China's monsoon variations are associated with planetary surface anomalies, including tropical Pacific sea surface temperature (SST), and Eurasian snow and soil moisture (Xu 1975; Fu and Teng 1988; Yang and Xu 1994; Liang et al. 1995a; Yang and Lau 1998). Strong associations have also been identified with the larger Asia monsoon system (Shukla 1987; Barnett et al. 1989; Webster and Yang 1992; Meehl 1994; Yang et al. 1996). However, these relationships result from nonlinear interactions of anomalous surface conditions with the dynamic circulation (Lau et al. 2000) and can change on decadal scales (Liang et al. 1995a). We will analyze the National Center for Atmospheric Research (NCAR) Community Climate Model, version 3 (CCM3; Kiehl et al. 1998), and the Climate System Model (CSM; Boville and Gent 1998) simulations to determine whether China's rainfall response to planetary surface forcing can be separated from internal variability and has decadal fluctuations.

2. Data

Observed precipitation is derived from a merged gauge–satellite archive, which has monthly records during 1979–98 on 2.5° grids (Xie and Arkin 1997). Model data are monthly averages and come from three separate sources: AMIP, CCM3, and CSM.

The AMIP set consists of simulations from 30 GCMs [see Phillips (1994) for model descriptions], where each integration has identically prescribed observed global SST evolution during 1979–88, insolation, and CO_2 concentration. This dataset is available from Lawrence Livermore National Laboratory/Program for Climate Model Diagnosis and Intercomparison (LLNL/PCMDI) and is used to explore whether a model with a realistic annual cycle can better predict interannual variability. Because each AMIP simulation employs a different initialization procedure, 1979 is considered to be a spinup period and is not used.

The CCM3 set contains 15 extended AMIP simulations using the NCAR CCM3 (Kiehl et al. 1998). The model was prescribed with three separate observed global SST archives constructed by the National Centers for Environmental Prediction (NCEP) Climate Analysis Center (CAC) and the Met Office (UKMO) where, for each archive, five individual integrations were conducted with different initial conditions (J. Lee 1999, personal communication; experimental design details are available online at http://www.cgd.ucar.edu/gds/jeff/jeff.html). In this study, we will utilize data from 1903 to 1994 for UKMO and from 1950 to 1997 for CAC and NCEP to identify robust SST-forced climate signals from internal variability.

The CSM set is the 300-yr equilibrium simulation of the current climate using the NCAR CSM, where CCM3 atmospheric and land processes are fully coupled with interactive global oceans (Boville and Gent 1998). We will analyze CSM output to explore decadal changes in China's rainfall response to planetary surface forcing. Both the CCM3 and CSM data have a T42 (~2.8°) horizontal resolution.

Because of observed and GCM spatial resolution differences as well as the dominant characteristics identified with east China's rainfall variations (see section 3), we consider latitude–time variations of zonally averaged features over 105°–122°E. Most AMIP GCMs adopt a grid mesh with a latitude interval of 2°–4°. Following Liang and Wang (1998), these zonal mean monthly precipitation values are calculated over 4° latitude bands with a 2° overlap (i.e., 28°–32°N, 30°–34°N, etc.). This overlap is intended to integrate optimally the fine structure information provided by high-resolution GCMs while broader band averages minimize the effects that result from coarse representations in lower-resolution models. Results for each band are obtained by areal averaging.

3. Dependence on the annual cycle

East China's rainfall is characterized by multiple monsoon onsets and latitudinal jumps. This occurs as the quasi-stationary major rainband advances rapidly from south (premonsoon, May) to central (mei-yu, June) and to north (July) China (Lau and Li 1984; Tao and Chen 1987; Lau et al. 1988; Samel et al. 1999). The duration of the prevailing rainfall system in each area is typically on the order of 1 month (Tao and Chen 1987; Samel et al. 1999). Relatively little precipitation falls during the remainder of the year. Thus, the above representation of east China's summer monsoon is adopted below to quantify the 1980–88 annual cycle and interannual variations, where summer is defined to be June–July–August (JJA).

Hovmöller (latitude–month) diagrams are constructed for the AMIP GCMs and observations over east China between 10° and 50°N during JJA. Each diagram contains a climatological rainfall pattern for the 22 overlapping bands, in order of increasing latitude and month (i.e., 22×3 points). Summer pattern correlations between the GCM and observed diagrams are calculated to determine model ability to simulate the climatological poleward march of monsoon rainfall. Interannual variability is assessed for the Yangtze River valley (25°–35°N), South China Sea (5°–20°N), and east China mainland (20°–45°N) subregions (see Fig. 1 for illustration of the key areas referred in this study). The first two have unique homogeneous climate characteristics and are identified with teleconnections (Yang and Xu 1994; Samel et al. 1995, 1999; Liang et al. 1995a; Liang and Wang 1998), and the latter is considered to illustrate results over a larger area. Given a specific subregion, a precipitation time series is constructed in order of increasing month and year (i.e., 3×9 points) for each

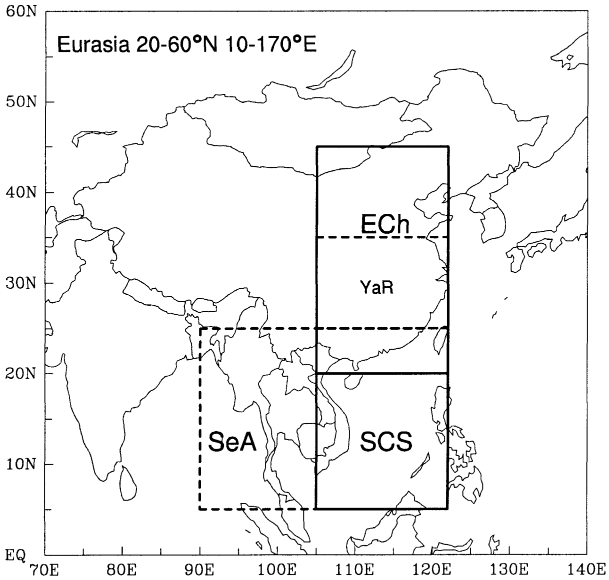

FIG. 1. The key areas referred to in this study including the east China mainland (ECh; 20°–45°N, 105°–122°E; top solid rectangle), the Yangtze River valley (YaR; 25°–35°N, 105°–122°E; top dashed rectangle within ECh), the South China Sea (SCS; 5°–20°N, 105°–122°E; bottom solid rectangle), Southeast Asia (SeA; 5°–25°N, 90°–122°E; bottom dashed rectangle), and a portion of Eurasia (20°–60°N, 10°–170°E).

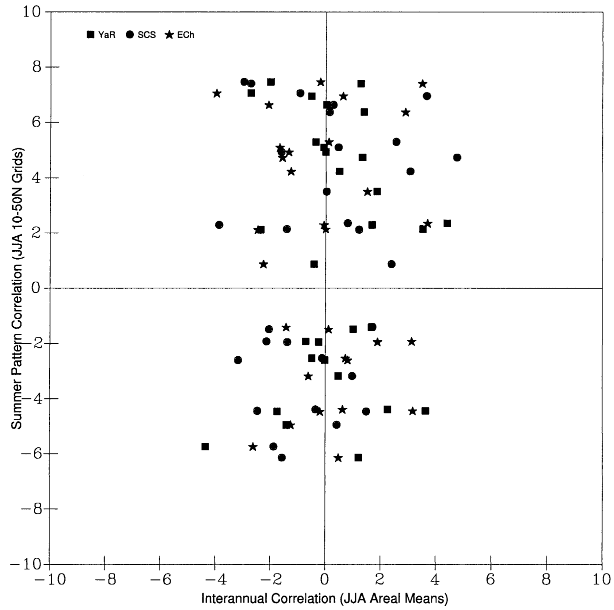

FIG. 2. Scatter diagram of correlations (× 10) between AMIP GCM simulated and observed mean summer rainfall patterns (1980–88) over east China and interannual variability over YaR (squares), SCS (dots), and ECh (stars). Note that there exists one (three) mean pattern (interannual variation) correlation(s) for each GCM.

model and for observations. Interannual correlations between observed and individual GCM series are calculated to determine the model predictive skill of regional summer monsoon interannual variability.

Summer pattern and interannual correlations are compared in Fig. 2 to explore whether a coherent relationship exists between the GCM's ability to reproduce the observed annual cycle and interannual variability of JJA precipitation. If all GCMs incorporate the same underlying mechanisms that couple the rainfall annual cycle and interannual variability components, the results should be clustered along a diagonal from the lower-left-hand to upper-right-hand corners of the plot. Models in the upper-right (lower left) corner most (least) realistically represent both components. On the other hand, models in the upper-left and lower-right corners reproduce only one component correctly and, hence, lack the coupling mechanisms. Models near the center point of the plot indicate no relationship with observations. The scattered nature of Fig. 2 indicates that there is clearly no systematic link between the GCM's ability to simulate the annual cycle and interannual variations over any of the subregions and that very few models realistically reproduce both components. Figure 2 compares pattern correlations over the east China domain with interannual values for the subregions; parallel plots of correlations calculated over the same subregions support the above conclusion.

The results show that accurate representation of the summer monsoon mean rainfall pattern does not ensure the realistic simulation of regional interannual variability. Conversely, models are not required to capture the annual cycle to depict interannual variability realistically. We believe, however, that a coherent relationship exists between model biases in the annual cycle and interannual variability when both components are governed by similar physical processes. For example, Liang and Wang (1998) showed that NCAR CCM3 produces an unrealistic east Asian jet stream and consequently fails to capture the east China monsoon. This relationship results from the dominant role of the jet stream on east China's rainfall in both the annual cycle (Liang et al. 2001) and interannual variability (Liang and Wang 1998).

4. Teleconnections with surface anomalies

A second fundamental issue is whether east China's rainfall interannual variability can be predicted from planetary surface anomalies. Observational and GCM studies have shown that Yangtze River valley and South China Sea precipitation is linked to tropical Pacific SST, Eurasian snow, and soil moisture anomalies (Xu 1975; Fu and Teng 1988; Yang and Xu 1994; Liang et al. 1995a; Yang and Lau 1998). Although both regions are relatively small and may not be sufficiently resolved by coarse-resolution GCMs, larger areas including the east China mainland and Southeast Asia (5°–25°N, 90°–122°E), have been linked with the above surface forcings (Webster and Yang 1992; Yang et al. 1996; Lau et al. 2000). These relationships result from nonlinear in-

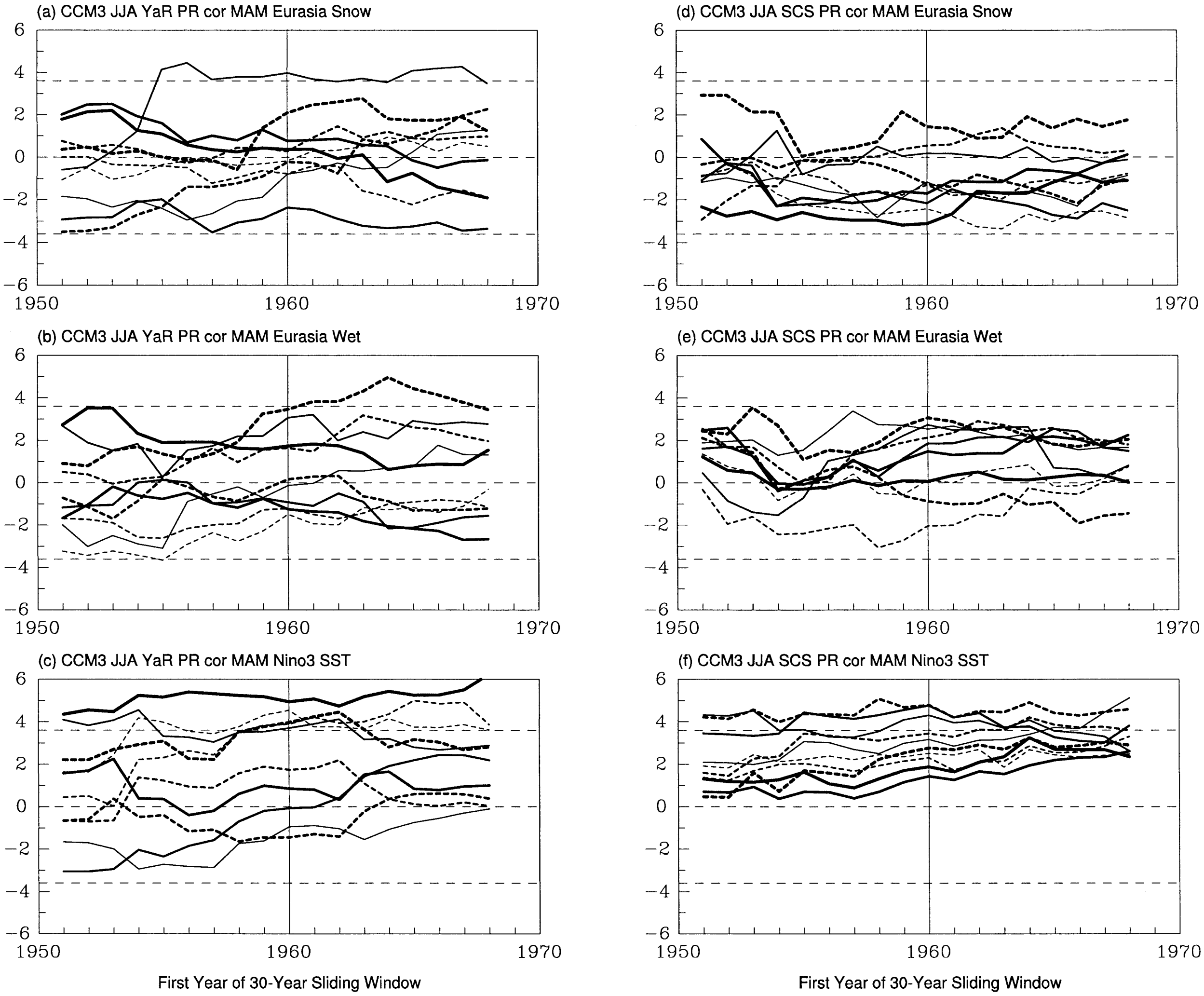

FIG. 3. CCM3 30-yr running correlations (× 10) between JJA YaR/SCS rainfall and preceding (a), (d) MAM Eurasian snow; (b), (e) soil moisture; and (c), (f) Niño-3 SST. Correlations are calculated for 1950–97, with individual values corresponding to the first year in the sliding window. The five solid (dashed) correlations in each panel correspond to ensembles using CAC (NCEP) global SST, with the realization number increasing with line thickness.

teractions of anomalous surface conditions with the dynamic circulation, can be masked by climate system internal natural variability (Fennessy and Shukla 1991; Palmer and Anderson 1994; Liang et al. 1997; Lau et al. 2000), and, thus, can change on decadal scales (Liang et al. 1995a). Therefore, we must distinguish forced climate signals from internal variability and identify decadal changes.

CCM3 ensemble integrations will be used in which, for each ensemble, individual realizations utilize identical global SST forcings and different initial conditions. Output will be analyzed to identify SST-forced signals from internal variability generated by initial condition differences. Like all AMIP GCMs, CCM3 has prescribed SST. Thus, air–sea interactions are not realistic, which may cause east China monsoon rainfall annual cycle biases, especially over the South China Sea (Liang et al. 2001). For this reason, we also analyze the CSM simulation, in which the atmosphere and oceans are fully coupled. East China's rainfall annual cycle is much more realistically depicted by the CSM for which summer pattern correlations are +0.6, whereas CCM3 values range from −0.3 to −0.1 for individual realizations. The longer CSM data records will also allow us to determine the signal robustness of decadal changes.

Thirty-year running correlations are calculated to determine regional rainfall teleconnections and their decadal changes (Liang et al. 1995b). For each consecutive 30-yr period, the first and last years of the time series are iterated by 1 year. Figure 3 shows running correlations of Yangtze River valley and South China Sea summer rainfall with preceding spring surface anomalies for the NCEP and CAC ensembles. All regional values are areal averages in which spring is defined as

March–April–May (MAM). The snow and soil moisture indices are computed over Eurasia (20°–60°N, 10°–170°E) and are often used to study monsoon teleconnections with continental surface conditions. The SST anomalies are calculated over the Niño-3 region (5°S–5°N, 90°–150°W) and are traditional measures for El Niño–Southern Oscillation (ENSO) variability.

The results show a large spread between realizations in the predictive skill of spring surface anomalies to determine Yangtze River valley and South China Sea summer rainfall, where coefficient amplitudes greater than 0.36 are significant at the 95% level, assuming 30–2 degrees of freedom.[1] Several realizations show stable signals over long periods, with persistent positive/negative or near-zero correlations. For example, Yangtze River valley precipitation and Eurasian snow cover correlations (Fig. 3a) are significantly positive after 1955 for the second CAC realization, are negative for the third CAC integration, and are near zero for the first NCEP simulation. On the other hand, correlations can change over time; for example, the fourth NCEP realization correlation increases from negative to positive. Both of these time-dependent characteristics can be generalized to correlations throughout Fig. 3. The results indicate that signals forced by surface anomalies, if any, are sensitive to initial conditions. If these signals are not a result of internal variability, then the underlying physical mechanisms must depend on specific dynamic regimes defined by the initial conditions. In addition, the individual ensembles have no systematic differences, which suggests that the use of different observed SST datasets has little impact on our findings. The longer UKMO ensemble (not shown) confirms these results and possesses clear evidence of decadal changes, which will be discussed below.

Figure 4 illustrates CSM 30-yr running correlations of Yangtze River valley, South China Sea, east China mainland, and Southeast Asia summer rainfall with preceding MAM surface anomalies. Statistically significant signals exist, but the teleconnections change on decadal scales. For example, Southeast Asia and South China Sea correlations with Eurasian snow cover are positive between model years 40–100, near zero afterward, and positive again during 190–240. Yangtze River valley correlations are positive from 5 to 35 but are negative between 120 and 170 and between 230 and 280; the unspecified years are not significant. Spring Eurasian soil moisture is positively correlated with Southeast Asia and South China Sea rainfall during 40–110 and again between 180 and 250; coefficients for the intermediate period are close to zero. Niño-3 SSTs are positively correlated with Yangtze River valley rainfall during 40–100, 130–170, and 210–280.

These results raise an important issue. If the fluctuations are not a manifestation of decadal change, then these regional variations cannot be predicted but instead are generated by climate system internal variability. In this regard, monsoon teleconnections identified in previous studies that used much shorter data periods may not be statistically significant and the hypotheses proposed to explain the underlying mechanisms cannot be generalized beyond the individual cases. On the other hand, if our results indicate a decadal teleconnection pattern change that is real, then the physical processes and underlying mechanisms must change accordingly. Liang et al. (1995a) found, in a 100-yr GCM simulation, three 30-yr periods when east China's rainfall variations were caused by distinct physical mechanisms associated with different planetary surface anomalies during the preceding spring. In the current study, model sensitivity to initial conditions limits predictability to certain climate regimes in which both teleconnections and physical mechanisms differ. We cannot, however, conclude which argument is correct because the observed data record is too short to perform a validation analysis.

5. Summary and discussion

This study investigated the dependence of China's rainfall interannual predictibility on the annual cycle and planetary surface anomalies. The results raise several important issues.

First, we found no coherent relationship between GCM ability to reproduce the observed annual cycle and interannual variability. Thus, accurate representation of the China summer monsoon mean rainfall pattern cannot ensure the realistic simulation of regional interannual variability. This, however, does not contradict previous studies, except when relationships between the mean state and interannual variations, if any, are stated in terms of the same field. We assert that a coherent link exists when the same physical processes govern both components. For example, the subtropical westerly jet plays a crucial role in effective Rossby wave source generation (Sardeshmukh and Hoskins 1988), and, thus, better representation of the mean jet will result in an improved interannual prediction of SST-forced extratropical responses (Kumar et al. 1996). The Indian monsoon strongly depends on ENSO processes, which must be better modeled to generate realistic interannual variability (Palmer and Mansfield 1986; Fennessy et al. 1994; Sperber and Palmer 1996; Gadgil and Sajani 1998; Sperber et al. 1999). Over China, the east Asian jet and Hadley cell mean states play crucial roles in the accurate depiction of both the monsoon annual cycle and interannual variability and must be improved to increase model overall performance (Liang and Wang 1998; Liang et al. 2001). Note, however, that the AMIP data period is too short to ascertain statistical robustness for interannual correlation patterns. We will revisit the issue by using AMIP II output (see online at http://

[1] We assume here that individual years are independent. However, because the exact degrees of freedom are difficult to determine, the term ''significance'' is used only as a guide, rather than to provide a strict threshold, to discriminate signals from noise.

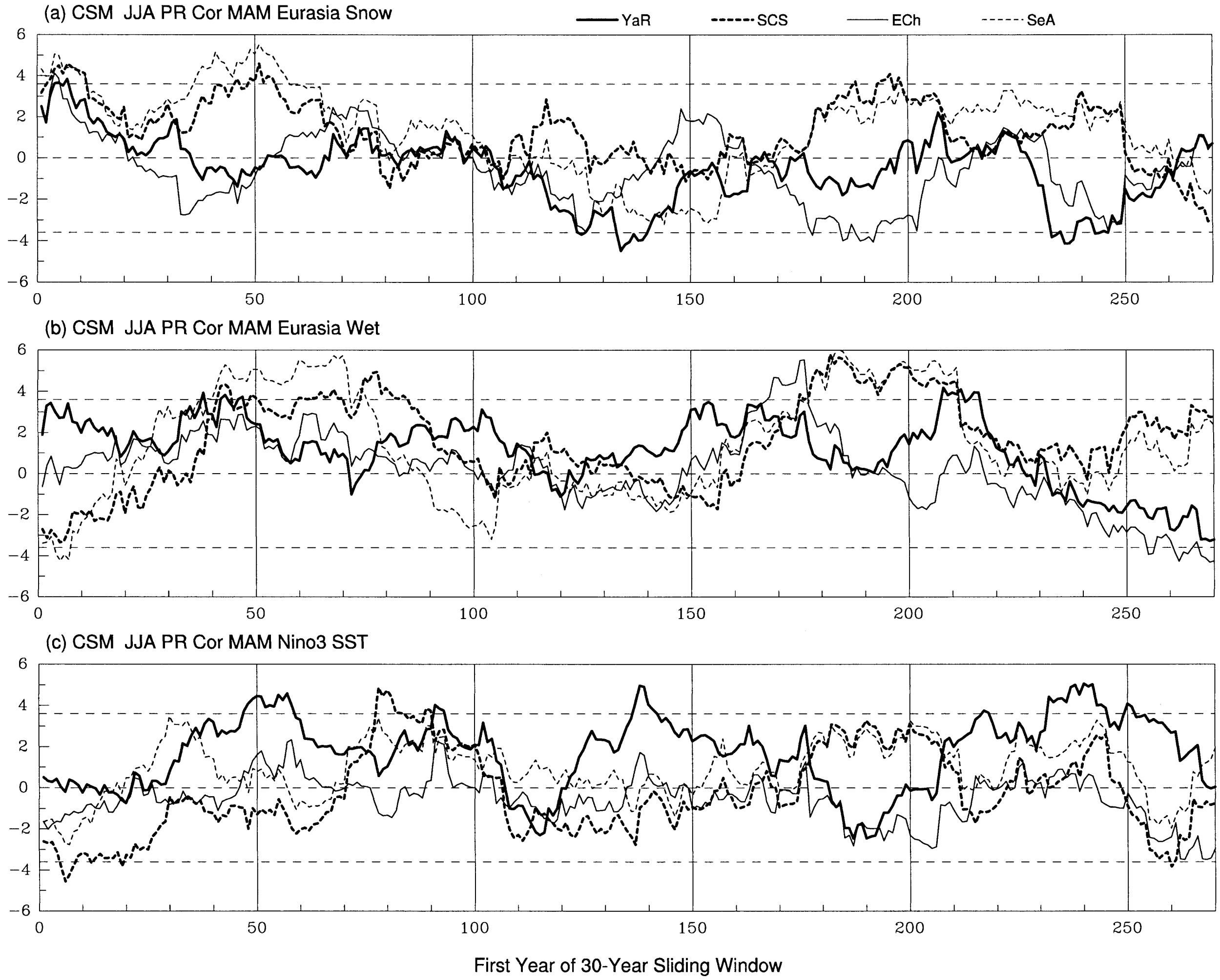

FIG. 4. CSM 30-yr running correlations (× 10) between JJA regional rainfall and preceding (a) MAM Eurasian snow, (b) Eurasian soil moisture, and (c) Niño-3 SST. Regions considered are YaR (heavy solid), SCS (heavy dash), ECh (light solid), and SeA (light dash).

www.pcmdi.llnl.gov/amip/), for which 1979–98 integrations with improved GCMs are available.

Second, we have demonstrated, using GCM simulations, that the impact of spring tropical Pacific SST and Eurasian snow and soil moisture anomalies on summer monsoon rainfall varies on decadal scales. This casts doubt on the physical mechanisms traditionally used to explain the corresponding teleconnections. Lacking an observational validation analysis, we speculate that decadal teleconnection pattern changes exist, in which the physical processes and underlying mechanisms change accordingly. In this study, because of model sensitivity to initial conditions, predictability applies only to certain climate regimes in which both teleconnections and physical mechanisms differ. This agrees with Lau et al. (2000) in that monsoon predictability depends on the slowly varying basic state and has decadal variations (Liang et al. 1995a; Mehta and Lau 1997).

We showed that CCM3 simulated interannual variations and decadal changes are very sensitive to initial conditions. Thus, it is unlikely that a direct comparison between a model ensemble mean and observations can determine GCM predictive skill. The conventional theory of ensemble mean predictability is based on the premise that SST anomalies are the dominant mechanism that causes climate variations in the study region. We have clearly shown that, over east China, this is typically not the case. Although SST anomalies may play a nontrivial role in regional climate predictability, this outcome requires correct specification of the dynamic circulation, which, in turn, is defined by the initial condition. However, systematic model biases and incomplete observations make realistic GCM initialization impossible at this time. Thus, subsequent GCM predictions based on SST anomalies may not be comparable with observations.

Acknowledgments. We thank the two anonymous reviewers for their comments and constructive suggestions. We acknowledge LLNL/PCMDI for making the

AMIP GCM results available and NCAR for the CCM3 and CSM simulations. We thank Drs. Kenneth Sperber, Song Yang, and Jeff Lee for their valuable comments and suggestions. This research is supported by two grants (to SUNYA) from the Office of Biological and Environmental Sciences of the Department of Energy and the Climate Dynamics Section of the National Science Foundation.

REFERENCES

Barnett, P. T., L. Dümenil, U. Schlese, E. Roeckner, and M. Latif, 1989: The effect of Eurasian snow cover on regional and global climate variations. *J. Atmos. Sci.,* **46,** 661–685.

Boville, B. A., and P. R. Gent, 1998: The NCAR Climate System Model, version one. *J. Climate,* **11,** 1115–1130.

Fennessy, M. J., and J. Shukla, 1991: Comparison of the impact of the 1982/83 and 1986/87 Pacific SST anomalies on time-mean predictions of atmospheric circulation. *J. Climate,* **4,** 407–423.

——, and Coauthors, 1994: The simulated Indian monsoon: A GCM sensitivity study. *J. Climate,* **7,** 33–43.

Fu, C. B., and X. L. Teng, 1988: The relationship between summer climate anomalies in China and El Niño–Southern Oscillation phenomena. *Sci. Atmos. Sin.,* 133–141.

Gadgil, S., and S. Sajani, 1998: Monsoon precipitation in the AMIP runs. *Climate Dyn.,* **14,** 659–689.

Gates, W. L., and Coauthors, 1999: An overview of the results of the Atmospheric Model Intercomparison Project (AMIP I). *Bull. Amer. Meteor. Soc.,* **80,** 29–55.

Kiehl, J. T., J. J. Hack, G. B. Bonan, B. A. Boville, D. L. Williamson, and P. J. Rasch, 1998: The National Center for Atmospheric Research Community Climate Model: CCM3. *J. Climate,* **11,** 1131–1149.

Kumar, A., M. Hoerling, M. Ji, A. Leetmaa, and P. Sardeshmukh, 1996: Assessing a GCM's suitability for making seasonal predictions. *J. Climate,* **9,** 115–129.

Lau, K.-M., and M. C. Li, 1984: The monsoon of East Asia and its global associations—A survey. *Bull. Amer. Meteor. Soc.,* **65,** 114–125.

——, G. J. Yang, and S. H. Shen, 1988: Seasonal and intraseasonal climatology of summer monsoon rainfall over East Asia. *Mon. Wea. Rev.,* **116,** 18–37.

——, K.-M. Kim, and S. Yang, 2000: Dynamical and boundary forcing characteristics of regional components of the Asian summer monsoon. *J. Climate,* **13,** 2461–2482.

Liang, X.-Z., and W.-C. Wang, 1998: Associations between China monsoon rainfall and tropospheric jets. *Quart. J. Roy. Meteor. Soc.,* **124,** 2597–2623.

——, A. N. Samel, and W.-C. Wang, 1995a: Observed and GCM simulated decadal variability of monsoon rainfall in east China. *Climate Dyn.,* **11,** 103–114.

——, W.-C. Wang, and M. P. Dudek, 1995b: Interannual variability of regional climate and its change due to the greenhouse effect. *Global Planet. Change,* **10,** 217–238.

——, K. R. Sperber, W.-C. Wang, and A. N. Samel, 1997: Predictability of SST forced climate signals in two atmospheric general circulation models. *Climate Dyn.,* **13,** 391–415.

——, W.-C. Wang, and A. N. Samel, 2001: Biases in AMIP model simulations of the east China monsoon system. *Climate Dyn.,* **17,** 291–304.

Meehl, G., 1994: Coupled land–ocean–atmosphere processes and south Asian monsoon variability. *Science,* **265,** 263–267.

Mehta, V., and K.-M. Lau, 1997: Influence of solar irradiance on the Indian monsoon–ENSO relationship at decadal–multidecadal time scales. *Geophys. Res. Lett.,* **24,** 159–162.

Palmer, T. N., and D. A. Mansfield, 1986: A study of wintertime circulation anomalies during past El Niño events using a high resolution general circulation model. I: Influence of model climatology. *Quart. J. Roy. Meteor. Soc.,* **112,** 613–638.

——, and D. L. T. Anderson, 1994: The prospects for seasonal forecasting—A review paper. *Quart. J. Roy. Meteor. Soc.,* **120,** 755–793.

Phillips, T. J., 1994: A summary documentation of the AMIP models. PCMDI Rep. 18, PCMDI, Lawrence Livermore National Laboratory, 343 pp.

Samel, A. N., S. Wang, and W.-C. Wang, 1995: A comparison between observed and GCM simulated summer monsoon characteristics over China. *J. Climate,* **8,** 1690–1696.

——, W.-C. Wang, and X.-Z. Liang, 1999: The monsoon rainfall period and interannual variability over China. *J. Climate,* **12,** 115–131.

Sardeshmukh, P. D., and B. J. Hoskins, 1988: The generation of global rotational flow by steady idealized tropical divergence. *J. Atmos. Sci.,* **45,** 1228–1251.

Shukla, J., 1987: Interannual variability of monsoons. *Monsoons,* J. S. Fein and P. L. Stephens, Eds., John Wiley and Sons, 399–463.

Sperber, K. R., and T. N. Palmer, 1996: Interannual tropical rainfall variability in general circulation model simulations associated with the Atmospheric Model Intercomparison Project. *J. Climate,* **9,** 2727–2750.

——, and participating AMIP modeling groups, 1999: Are revised models better models? A skill score assessment of regional interannual variability. *Geophys. Res. Lett.,* **26,** 1267–1270.

Tao, S.-Y., and L.-X. Chen, 1987: A review of recent research of the east Asian summer monsoon in China. *Monsoon Meteorology,* C.-P. Chang and T. N. Krishnamurti, Eds., Oxford University Press, 60–92.

Wang, W.-C., and Coauthors, 1998: GCM simulations of the east Asia climate. *Proceedings of the Third East Asia–West Pacific Meteorology and Climate Conference,* C.-P. Chang, Ed., World Scientific Publication Corp., 473–482.

Webster, P. J., and S. Yang, 1992: Monsoon and ENSO: Selectively active systems. *Quart. J. Roy. Meteor. Soc.,* **118,** 877–926.

Xie, P., and P. A. Arkin, 1997: A 17-year monthly analysis based on gauge observation, satellite estimates, and numerical model outputs. *Bull. Amer. Meteor. Soc.,* **78,** 2539–2558.

Xu, Q., 1975: Mei-Yu (monsoon rainfall) in the Yangtze River valley during the last 80 years. *Acta. Meteor. Sin.,* **33,** 507–518.

Yang, S., and L. Xu, 1994: Linkage between Eurasian winter snow cover and regional Chinese summer rainfall. *Int. J. Climatol.,* **14,** 739–750.

——, and K.-M. Lau, 1998: Influences of sea surface temperature and ground wetness on Asian summer monsoon. *J. Climate,* **11,** 3230–3246.

——, ——, and M. Samkar-Rao, 1996: Precursory signs associated with the interannual variability of the Asian summer monsoon. *J. Climate,* **9,** 949–964.